

## Electron Microscopic Study of Interdiffusion in Equiatomic Fe–Ni Composite

V.V. BOGDANOV<sup>a</sup>, R.V. VOVK<sup>a</sup>, S.V. DUKAROV<sup>a</sup>, M.V. KISLITSA<sup>a</sup>,  
S.I. PETRUSHENKO<sup>a</sup>, V.N. SUKHOV<sup>a</sup>, G.YA. KHADZHAI<sup>a</sup>,  
Y.L. GOULATIS<sup>a</sup>, S.R. VOVK<sup>b,c</sup>, E.S. GEVORKYAN<sup>b</sup>, A. FEHER<sup>c</sup>,  
P. KOLLAR<sup>c</sup>, J. FUZER<sup>c</sup> AND J.N. LATOSIŃSKA<sup>d,\*</sup>

<sup>a</sup>*V.N. Karazin Kharkiv National University, 4 Svobody Sq., Kharkiv 61022, Ukraine*

<sup>b</sup>*Ukrainian State University of Railway Transport, 7 Feierbakh Sq., Kharkiv 61050, Ukraine*

<sup>c</sup>*Centre of Low Temperature Physics, Faculty of Science, P.J. Safarik University,  
Park Angelinum 9, 041 54 Kosice, Slovakia*

<sup>d</sup>*Adam Mickiewicz University, Uniwersytetu Poznańskiego 2, 61-614 Poznań, Poland*

Received: 12.08.2020 & Accepted: 14.10.2020

Doi: [10.12693/APhysPolA.139.62](https://doi.org/10.12693/APhysPolA.139.62)

\*e-mail: [jolanta.latosinska@amu.edu.pl](mailto:jolanta.latosinska@amu.edu.pl)

The paper presents a study of interdiffusion processes in a binary Fe–Ni system (obtained by electroconsolidation of nickel and iron powders) by X-ray energy dispersive spectroscopy. Well-separated regions of almost pure iron and nickel have been discovered. The content of nickel, estimated from the concentration dependence of the interdiffusion coefficient, which determines the kinetics of the homogenization process of the electroconsolidated Fe–Ni composite sample, was  $\approx 70$  at.%. The value of the interdiffusion coefficient of the electroconsolidated Fe–Ni composite is significantly higher than that of the alloy of similar composition which probably results from the effect of spark plasma sintering technology (pressure and current along the same direction during consolidation) but also from a significant contribution of diffusion with mass transfer along the particle boundaries in the composite.

topics: Fe–Ni binary system, electron microscopy, interdiffusion processes, spark plasma sintering technology and mass transfer effect

### 1. Introduction

Binary metallic systems are important in modern technology as they are widely used in metallurgy and for specialized high-tech applications. In this regard, the Fe–Ni system combines the availability of components and specific properties. This binary system is used in modern technologies, e.g., as a matrix for OLED displays, which has stimulated research in the direction of improving the electrodeposition methods of this alloy [1, 2]. The use of Fe–Ni-based composite structures is widespread, e.g., as protective coatings [3], basis for catalysts used in plastic processing [4, 5], water splitting [6–9] and hydrogen storage [10, 11]. Notably, Fe–Ni, along with other bimetallic systems [12], is considered as a bifunctional element for the extraction and reduction of oxygen in fuel cells and air-zinc accumulators [13]. Highly ordered Fe–Ni alloys (the so-called tetraenaite ordered) are regarded as an affordable alternative to modern powerful magnets made on the basis of rare-earth materials [14, 15].

It should be noted that, despite a wide development of various, primarily electrochemical, methods

of obtaining structures based on Fe–Ni, metallurgical methods, in particular sintering, continue to be the basis of many modern technologies.

Electroconsolidation technologies, such as field activated sintering technique (FAST) and spark plasma sintering (SPS) [16], are very effective for the manufacture of composites of hardly sintering materials and compounds. In such technologies, electric current is passed along the applied external pressure, generating considerable heat (both field and direct effect), making it possible to significantly accelerate heating and reduce the sintering time to several minutes. In such short processes, large crystalline grains do not have time to form, that is, compaction is faster than grain growth [17] and thereby a high-density and finely dispersed composite structure [18] is ensured.

During consolidation, mass transfer by surface and bulk diffusion as well as plastic deformation are activated by temperature which during electroconsolidation is within  $0.5T_{\text{melt}} < T_{\text{sint}} < T_{\text{melt}}$  [19]. At the sites of point contacts of grains, they deform and the area of the boundaries increases many times which also increases mass transfer.

Electro-discharge processes occur along grain boundaries which accelerates consolidation due to local welding of powder particles and additional mass transfer due to internal temperature gradients in the composite under the influence of inhomogeneous electric current density between pores [20].

Local plasma formation as a result of electric discharges leads to the cleaning and activation of the surface of sintered powders which significantly contributes to the chemical purity of the final product and compaction of sintered powders [21].

At the same time, diffusion processes occurring in the Fe–Ni binary system both during its production and during its operation have not been studied enough, especially since the diffusion processes finally determine not only the possibility of forming structures with specified functional properties but also their safety over time.

In this work, we study the concentration dependence of the diffusion coefficient in Fe–Ni samples obtained by electroconsolidation (SPS).

## 2. Experiment

The samples were obtained by electroconsolidation of nickel and iron powders for 10 min at a temperature of 1100°C, a pressure of 35 MPa and a current of  $\approx 5$  kA. The heating rate was  $\approx 200^\circ\text{C}/\text{min}$ . The studied sample of the composite had the shape of a bar with a rectangular cross section with dimensions  $15 \times 4 \times 6 \text{ mm}^3$ .

The surface was carefully polished and examined using a Tescan Vega 3LMH scanning electron microscope (SEM) equipped with a Bruker X Flash 5010 EDS characteristic X-ray detector.

The elemental composition was determined in the detector self-calibration mode. To determine the spatial distribution of the elements, the sample was scanned in the direction parallel or perpendicular to that of the electric current passing through the sample and the pressure applied during sintering. The spatial step of the probe during the transition from one scanning point to another was 1 or 2  $\mu\text{m}$  and the signal accumulation time from one point was usually chosen as 32 s. For all elements except iron and nickel, the “deconvolution only” mode was selected. To take into account a possible influence of the initial particle shape and surface effects on

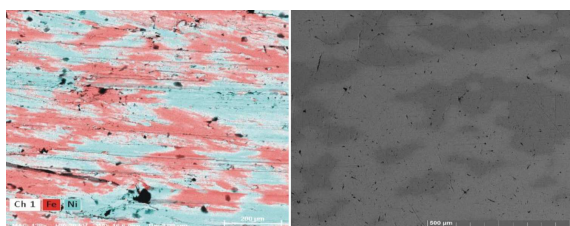


Fig. 1. Results of elemental mapping (left) and SEM image (right, BSE mode) of an Fe–Ni composite sample obtained by electroconsolidation.

the mass transfer of matter, in a separate series of experiments, the electron probe was sequentially passed along the same line on the sample surface using different accelerating voltage values. Since the penetration depth of electrons and, consequently, the generation region of the characteristic X-ray signal strongly depend on the initial electron energy, this procedure permitted gaining some information about the influence of the form factor on diffusion processes in the sample.

## 3. Results and discussion

Figure 1 shows the map of distribution of elements and SEM images of an Fe–Ni sample after sintering. It can be seen that it is a two-phase sample, with clearly separated regions of almost pure iron and nickel. The contrast between the phases is well-observed not only in a backscattered electron (BSE) but also in a secondary electron (SE) mode. It is probably due to a different hardness of nickel and iron which causes morphological contrast during polishing.

A typical dependence of the concentration of nickel (or iron) on the coordinate of the probe is shown in Fig. 2. The left edge of the SEM image was taken as a reference point. The frame size and its location were chosen in such a way as to capture the areas of phase zones free from the second component (see Fig. 3).

Figure 4 presents the results of constructing the distribution of elements along the scan line obtained at different accelerating voltage. Scanning was carried out along the same line, without moving the sample (see Fig. 3). Figure 4 gives some idea of the distribution of elements along the depth of the sample. It can be seen that, in the central region of the distribution, the difference between the concentrations obtained at the same point of the sample at probe energies of 15 and 30 keV reaches 20–25 at. frac. For comparison, we indicate that for the dependences obtained at the same accelerating

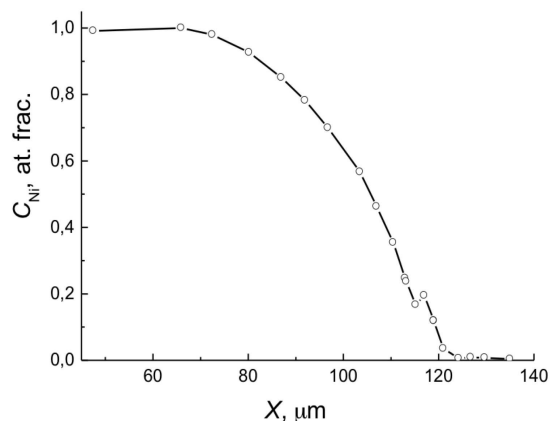


Fig. 2. Dependence of nickel concentration on the coordinate along the scan line.

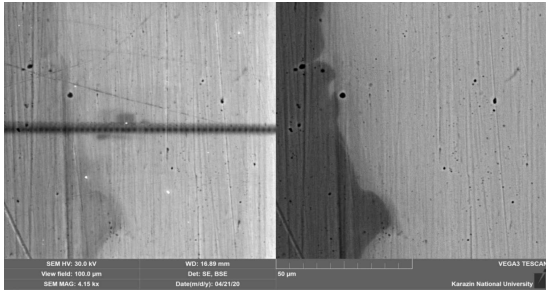


Fig. 3. Cropping example to obtain a series of energy dispersive X-ray spectra (EDS). The SE image shows the effects of carbon pollution, stimulated by the multiple passage of an electron beam.

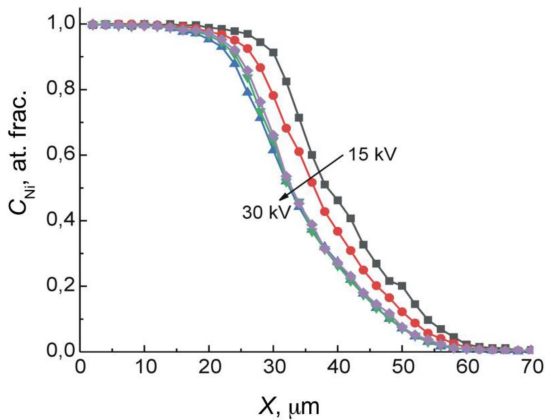


Fig. 4. The coordinate dependences of the iron concentration obtained at different energies of the electron probe.

voltage during successive scanning cycles, this difference is only 1–2% and is random. The observed effect may be due to the peculiarities of the distribution of matter in a narrow layer on the grain surface, which can have a decisive influence on the behavior of nanocomposite structures. The studies in [15] have shown that, due to the size dependence of the diffusion coefficient, the synthesis of functional structures of the L10 phase type Fe–Ni turned out to be possible at a temperature of only 320°C. However, a detailed explanation of this phenomenon needs a separate study.

To obtain the concentration dependence of the diffusion coefficient, we used the data obtained at the probe energy of 30 keV. As it can be seen in Fig. 4, with increasing the probe energy, the experimental dependences asymptotically approach those obtained at the accelerating voltage of 30 kV. Apparently, they characterize the diffusion processes occurring in the bulk of the sintered material.

Using the Boltzmann–Matano method, we calculated the concentration dependence of the interdiffusion coefficient ( $C$ ) from the  $C_{Ni}(x)$  curve (Fig. 2) [22]. The results of calculations of the diffusion coefficient concentration dependence are presented in Fig. 5. Notably, we did not find a significant effect of the passage direction of the probe

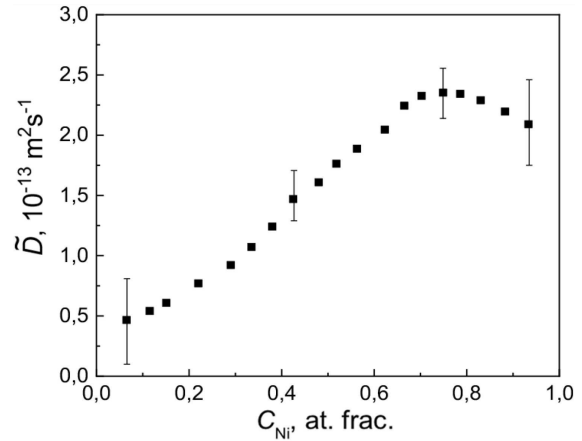


Fig. 5. The concentration dependence of the interdiffusion coefficient  $\tilde{D}(C_{Ni})$  in the Fe–Ni composite.

(relative to the direction of transmission of the current applied during sintering) on the value of the diffusion coefficient.

The  $C$  dependence has the form of a smooth curve with a maximum in the region of  $\approx 70$  at. % Ni, according to the literature data for the interdiffusion coefficient in the Fe–Ni system (see, e.g., [23–26]) and is correlated with the concentration dependence of the partial coefficients diffusion of components in the Fe–Ni binary alloy with unlimited component solubility.

The maximum in the  $C$  dependence is associated with the shape of the equilibrium diagram for the Fe–Ni binary system [27], in which the liquidus and solidus curves for alloys with a content of 5.9–100 at.%Ni have the form of a sagging chain with a minimum at 1436°C and a content of 68 at.%Ni. As known, the diffusion of atoms in an alloy of variable concentration is the higher, the lower the melting temperature of the alloy [28]. That is the reason why the interdiffusion coefficient of the alloy concentration  $\approx 70$  at.%Ni has a maximum value.

However, the diffusion coefficient obtained here is much higher than in the literature [23–26]. For instance, in [24],  $\tilde{D}(1100^\circ\text{C}) = 3.2 \times 10^{-15} \text{ m}^2/\text{s}$ . High values of diffusion coefficients can be associated with the impact of the electric current flowing through particles of Fe and Ni. The current causes local heating and cleaning of the surface of the particles which activates the diffusion process. In addition, due to a large area of interparticle (interphase) boundaries in the composites, the diffusion mass transfer along the boundaries can become pivotal.

#### 4. Conclusions

Concentration dependence of the interdiffusion coefficient, which determines the kinetics of the homogenization process of an electroconsolidated Fe–Ni composite sample, was obtained by EDS.

The indicated dependence has a maximum at a nickel content of  $\approx 70$  at.%. This is similar to the concentration dependence of the interdiffusion coefficient in Fe–Ni alloys.

The value of the interdiffusion coefficient in an electroconsolidated Fe–Ni composite is significantly larger than in an alloy of a similar composition which indicates the probable effect of SPS technology (pressure and current along one direction during consolidation) together with a significant contribution in mass transfer of diffusion along the particle boundaries in the composite.

### References

- [1] A. Li, Z. Zhu, Y. Liu, J. Hu, *Mater. Res. Bull.* **127**, 110845 (2020).
- [2] T. Nagayama, T. Yamamoto, T. Nakamura, in: *SID Symp. Digest of Technical Papers*, Vol. 48, 2017, p. 527.
- [3] J. Liu, H. Liu, X. Tian, H. Yang, J. Hao, *J. Alloys Compd.* **822**, 153708 (2020).
- [4] T. Chen, J. Yu, C. Ma, K. Bikane, L. Sun, *Chemosphere* **248**, 125964 (2020).
- [5] N. Cai, H. Yang, X. Zhang, S. Xia, D. Yao, P. Bartocci, P.T. Williams, *Waste Manage.* **109**, 119 (2020).
- [6] Z. Zhang, L. Cong, Z. Yu, L. Qu, W. Huang, *Mater. Today Energy* **16**, 100387 (2020).
- [7] Y. Wu, Y. Yi, Z. Sun, H. Sun, T. Guo, M. Zhang, J. Sun, *Chem. Eng. J.* **390**, 124515 (2020).
- [8] A. Fan, C. Qin, X. Zhang, J. Yang, J. Ge, S. Wang, X. Dai, *J. Mater. Chem. A* **7**, 24347 (2019).
- [9] G. Zhang, G. Wang, H. Liu, J. Qu, J. Li, *Nano Energy* **43**, 359 (2018).
- [10] L. Ji, L. Zhang, X. Yang, X. Zhu, L. Chen, *Dalton Trans.* **49**, 4146 (2020).
- [11] S. Gao, H. Wang, X. Wang, H. Liu, T. He, Y. Wang, M. Yan, *J. Alloys Compd.* **830**, 154631 (2020).
- [12] S. Sarkar, A. Biswas, T. Purkait, M. Das, N. Kamboj, R.S. Dey, *Inorg. Chem.* **59**, 5194 (2020).
- [13] X. Zhu, D. Zhang, C.J. Chen, Q. Zhang, R.S. Liu, Z. Xia, X. Lu, *NanoEnergy* **71**, 104597 (2020).
- [14] S. Goto, H. Kura, E. Watanabe, Y. Hayashi, H. Yanagihara, Y. Shimada, E. Kita, *Sci. Rep.* **7**, 1 (2017).
- [15] V.L. Kurichenko, D.Y. Karpenkov, A.Y. Karpenkov, M.B. Lyakhova, V.V. Khovaylo, *J. Magn. Magn. Mater.* **470**, 33 (2019).
- [16] F. Bernard, S. Le Gallet, N. Spinassou, S. Paris, E. Gaffet, J.N. Woolman, Munir Z.A., *Sci. Sinter.* **36**, 155 (2004).
- [17] G.S. Upadhyaya, *Powder Metallurgy Technology*, Cambridge Int. Sci. Publ., 1996.
- [18] D.L. Bourell, J.R. Groza, in: *Powder Metallurgy. ASM Handbook*, 1998, Vol. 7, p. 504.
- [19] Ya.E. Geguzin, *Physics of Sintering*, 2nd ed., Nauka, Moscow 1984 (in Russian).
- [20] V.Y. Kodash, J.R. Groza, K.C. Cho, B.R. Klotz, R.J. Dowding, *Mater. Sci. Eng. A* **385**, 367 (2004).
- [21] E. Aslan, N. Camuşcu, B. Birgören, *Mater. Des.* **28**, 1618 (2007).
- [22] B.S. Bokshstein, *Diffusion in Metals*, Metallurgy, Moscow 1978 (in Russian).
- [23] A. Kohn, J. Levasseur, J. Philibert, M. Wanin, *Acta Metall.* **18**, 163 (1970).
- [24] Yu.E. Ugaste, A.A. Kodenczov, F. van Loo, *Phys. Met. Metall.* **88**, 88 (1999) (in Russian).
- [25] M. Badia, Ph.D. Thesis, Univ. Nancy, 1969.
- [26] J.I. Goldstein, R.E. Hanneman, R.E. Ogilvie, *Trans. Metall. Soc. AIME* **233**, 812 (1965).
- [27] L.J. Swartzendruber, V.P. Itkin, C.B. Alcock, *J. Phase Equilib.* **12**, 288 (1991).
- [28] J. Philibert, *Atom Movements. Diffusion and Mass Transport in Solids*, Les Editions de Physique, France 1991.